Available online at www.sciencedirect.com

ScienceDirect

Polymer 48 (2007) 6481–6490

polymer

www.elsevier.com/locate/polymer

Synthesis and properties of carbazole-based hyperbranched conjugated polymers

Jinqing Qu [a], Masashi Shiotsuki [a], Norihisa Kobayashi [b], Fumio Sanda [a,*], Toshio Masuda [a,*]

[a] *Department of Polymer Chemistry, Graduate School of Engineering, Kyoto University, Katsura Campus, Kyoto 615-8510, Japan*
[b] *Department of Information and Image Sciences, Chiba University, Chiba 263-8522, Japan*

Received 24 May 2007; received in revised form 30 August 2007; accepted 5 September 2007

Abstract

Carbazole-based novel hyperbranched conjugated polymers linked with triphenylamine and benzene moieties were synthesized by Sonogashira coupling polycondensation of *N*-octadecyl- and *N*-octyl-3,6-diethynylcarbazoles with tris(4-iodophenyl)amine and 1,3,5-tribromobenzene. Solvent-soluble polymers with number-average molecular weights in the range of 3500–21,000 were obtained in 48–66% yields. The UV–vis absorption bands of the polymers were red-shifted compared to that of carbazole, indicating the extension of conjugation length. The polymers emitted blue–green fluorescence with high quantum yields up to 67% in $CHCl_3$. Poly(**1/3**) containing triphenylamine units emits visible light and shows unique solvatochromism. The polymers were electrochemically redox-active.

Keywords: Carbazole; Conjugated polymer; Hyperbranched polymer

1. Introduction

Polymers containing carbazole moieties in the main chain or side chain have attracted much attention because of their unique properties derived from carbazole [1], which allow them to be applied to various photonic materials such as photoconductive, electroluminescent, and photorefractive materials [2]. Polyvinylcarbazole is a representative functional polymer carrying carbazole in the side chain. Polyacetylenes with pendent carbazole have also been investigated, some of which exhibit photoluminescence, photoconductivity, and electroluminescence, as expected from the conjugated main chain along with the carbazole side chain [3–5]. On the other hand, conjugated polymers containing carbazole in the main chain have also been extensively studied, which include polycarbazoles [6], polycarbazolyleneethynylenes [7], and polycarbazolylenevinylenes [8]. Carbazole-containing poly(arylenevinylenes) emit blue-green fluorescence with high quantum yields [9]. Most of these polymers containing carbazole in the main chain form aggregates under certain conditions, because of intense π-stacking nature of carbazole units [10]. Aggregation of polycarbazoles leads to formation of weakly emissive interchain species in thin films, which significantly reduces the luminescence quantum efficiency [11]. Spherical shaped molecules cannot regularly stack in a side-by-side fashion, and thus they are exempted from aggregate-based fluorescence quenching [12]. Hyperbranched polymers are spherical shaped molecules, and have recently gathered increasing attention both in scientific and industrial fields due to their unique molecular architecture. They show excellent optical properties such as high light-emitting efficiency, superb optical-limiting performance, processability, thermal resistance, and morphological stability [13,14].

Polymeric and oligomeric materials based on triphenylamine as well as carbazole are important organic semiconductors that are applicable to hole-transporting materials in thin layer electrooptical devices such as organic light-emitting

---

* Corresponding authors.
E-mail addresses: sanda@adv.polym.kyoto-u.ac.jp (F. Sanda), masuda@adv.polym.kyoto-u.ac.jp (T. Masuda).

0032-3861/$ - see front matter © 2007 Elsevier Ltd. All rights reserved.
doi:10.1016/j.polymer.2007.09.011

diodes, solar cells, organic field effect transistors, two-photon micro/nanolithography, and photorefractive holography [15]. Consequently, incorporation of carbazole or triphenylamine into hyperbranched polymers hopefully leads to the development of optically and electronically functional novel polymers [16]. However, hyperbranched polymers carrying carbazole and triphenylamine have been scarcely investigated to the best of our knowledge. In the present paper, we disclose the synthesis of carbazole-based novel hyperbranched polymers linked with triphenylamine and benzene moieties [poly(**1**/**3**)–poly(**2**/**4**)] as illustrated in Scheme 1, and examination of the optical and electrochemical properties. We also discuss the effect of aggregation on the optical properties.

2. Experimental

2.1. Measurements

^{1}H (400 MHz) and ^{13}C (100 MHz) NMR spectra were recorded on a JEOL EX-400 spectrometer using tetramethylsilane as an internal standard. IR, UV–vis, and fluorescence spectra were measured on JASCO FTIR-4100, V-550, and FP750 spectrophotometers, respectively. The number- and weight-average molecular weights (M_n and M_w) of polymers were determined by gel permeation chromatography (GPC) on a JASCO GULLIVER system (PU-980, CO-965, RI-930, and UV-1570) equipped with polystyrene gel columns (Shodex columns K804, K805, and J806), using THF as an eluent at a flow rate of 1.0 mL/min, calibrated by polystyrene standards at 40 °C, and GPC right-angle laser light scattering (RALLS) on a Viscotek T-60A eluted with THF at 40 °C. Cyclic voltammograms were measured on an HCH Instruments electrochemical analyzer ALS600A-n. The measurements were carried out with a glassy carbon rod as the working electrode coupled with a Pt plate counter and an Ag/AgCl reference electrode, with a solution of a polymer (0.5 mg/mL) and tetrabutylammonium perchlorate (0.1 M) in $CHCl_3$.

2.2. Evaluation of photoconductivity

A 5 wt% solution of a polymer in THF was cast on an ITO electrode and then dried for 12 h in vacuo to prepare a thin film with a thickness of 6 μm. Au was vacuum evaporated to prepare a counter electrode for the ITO electrode. The relationships between current (I) and applied voltage (V) for the ITO/the polymer film/Au cells (effective electrode area 0.12 cm^2) were measured at room temperature under reduced pressure of 10^{-2} Torr in the dark and under

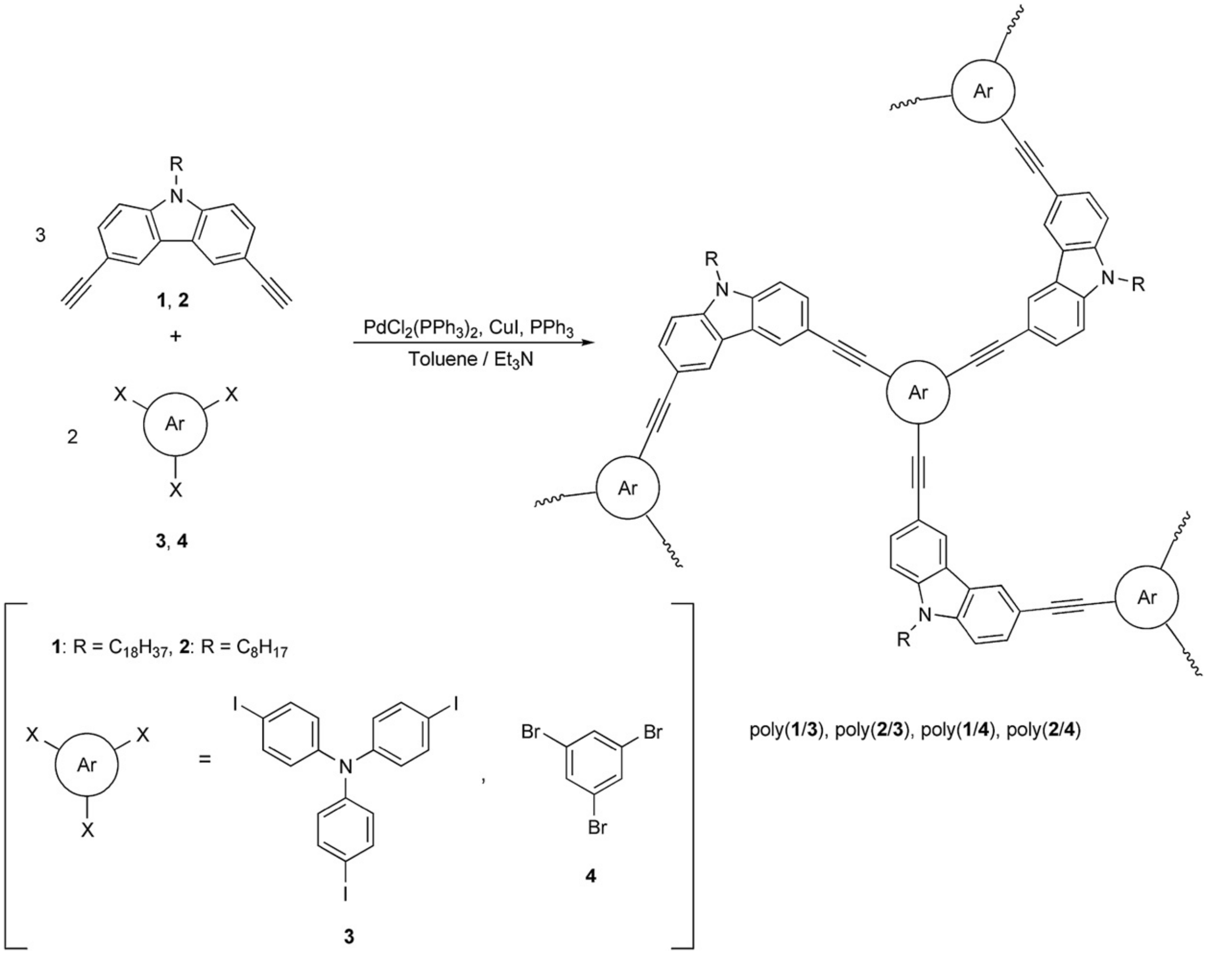

Scheme 1. Polycondensation of *N*-alkyl-3,6-diethynylcarbazoles **1** and **2** with tris(4-iodophenyl)amine (**3**) and 1,3,5-tribromobenzene (**4**).

photoillumination (2.5 mW/m^2) with a Xe lamp using a thermoabsorption filter.

2.3. Materials

N-Octadecyl-3,6-diethynylcarbazole (**1**) and *N*-octyl-3,6-diethynylcarbazole (**2**) were synthesized according to the literature [9]. Tris(4-iodophenyl)amine (**3**) and 1,3,5-tribromobenzene (**4**) were purchased from TCI and Aldrich, respectively, and used as received. The solvents used for polymerization were purified by standard methods.

2.4. Polycondensation

The polycondensation of diethynylcarbazoles with trihaloarenes was conducted in a Schlenk tube under nitrogen. *N*-Octadecyl-3,6-diethynylcarbazole (140 mg, 0.30 mmol), tris(4-iodophenyl)amine (125 mg, 0.20 mmol), $PdCl_2(PPh_3)_2$ (4.0 mg, 0.005 mmol), CuI (3.7 mg, 0.02 mmol), and PPh_3 (7.6 mg, 0.030 mmol) were added to a mixture of toluene/Et_3N (9:1, v/v) (5 mL), and the resulting mixture was stirred at 30 °C for 72 h. Et_3N and toluene were removed from the mixture by evaporation, then the obtained material was washed with water, dissolved in a small amount of $CHCl_3$, and then the mixture was filtered. The filtrate was poured into a large amount of acetone to precipitate a polymer. It was further purified by repeated precipitation, isolated by filtration, and dried under reduced pressure. Yield of 54% is obtained. The other polymers were synthesized in a similar manner.

2.5. Spectroscopic data of polymers

Poly(**1/3**): ^{1}H NMR (400 MHz, in ppm, $CDCl_3$): 0.78–1.75 (m, 35H, $C_{17}H_{35}$), 4.17 (broad s, 2H, NCH_2), 7.02–8.17 (m, 18H, Ar). IR (KBr): 3458, 3036, 2921, 2850, 2204, 1598, 1560, 1542, 1505, 1482, 1466, 1381, 1317, 1283, 880, 830, 800, 728, 669 cm^{-1}. Poly(**2/3**): ^{1}H NMR (400 MHz, in ppm, $CDCl_3$): 0.82–1.85 (m, 15H, C_7H_{15}), 4.21 (broad s, 2H, NCH_2), 6.83–8.39 (m, 18H, Ar). IR (KBr): 3433, 3035, 2923, 2852, 2202, 1597, 1505, 1482, 1381, 1348, 1316, 1283, 1226, 879, 830, 803, 726, 652 cm^{-1}. Poly(**1/4**): ^{1}H NMR (400 MHz, in ppm, $CDCl_3$): 0.87–1.86 (m, 35H, $C_{17}H_{35}$), 4.29 (broad s, 2H, NCH_2), 7.29–8.25 (m, 9H, Ar). IR (KBr): 3434, 2936, 2852, 2207, 1598, 1560, 1509, 1475, 1433, 1398, 1383, 1170, 1035, 849, 804, 721, 652 cm^{-1}. Poly(**2/4**): ^{1}H NMR (400 MHz, in ppm, $CDCl_3$): 0.83–1.79 (m, 15H, C_7H_{15}), 4.15 (broad s, 2H, NCH_2), 7.00–8.17 (m, 9H, Ar). IR (KBr): 3421, 3049, 2923, 2852, 2204, 1597, 1547, 1509, 1484, 1466, 1381, 1349, 1285, 1224, 1149, 1131, 879, 860, 804, 723, 652 cm^{-1}.

3. Results and discussion

3.1. Polycondensation

Table 1 summarizes the conditions and results of the polycondensation of A_2-monomers **1** and **2** with B_3-monomers **3** and **4** catalyzed by $PdCl_2(PPh_3)_2$–PPh_3–CuI. The polymerization mixtures of monomers **1/3** and **2/3** became pale yellow in 3 h, and gradually turned into brown accompanying appearance of solvent-insoluble white acicular solid. The polymerization mixtures kept transparency throughout the reaction. After 72 h, the mixture was passed through a cotton filter and poured into acetone to isolate a soluble product. When we raised the monomer concentrations twice as large as those of Table 1 keeping the mole ratios of **1/3** and **2/3** at 3:2, the polymerization mixtures did not keep transparency, and the amount of insoluble part in $CHCl_3$ increased, leading to the decrease of the $CHCl_3$-soluble polymer yields. On the other hand, the polymerization mixture of monomers **1/4** and **2/4** became orange 12 h after initiation, and gradually turned into dark orange accompanying appearance of solvent-insoluble solids. The polymerization temperature affected the polymerization of monomers **1/4** and **2/4**. Namely, when the temperature was raised to 80 °C in the polycondensation of **1** and **2** with **4**, a large amount of solvent-insoluble polymers was formed in a short period, presumably because the reaction went out of control to yield networks. After reaction for 30 h, the polymers were obtained in 48–66% yields. The low yields were due to removal of solvent-insoluble parts (about 15%) by filtration. The M_ns of the polymers estimated by GPC with UV detection calibrated by polystyrene were in the range of 3500–21,000, while those estimated by GPC-

Table 1
Polycondensation of A_2-monomers **1** and **2** with B_3-monomers **3** and **4**[a]

Run	A_2-monomer/B_3-monomer	Temp (°C)	Polymer[b]					
			Yield (%)	GPC-UV		GPC-RALLS		Unit ratio of A_2-monomer/B_3-monomer (r)[e]
				M_n[c]	M_w/M_n[c]	M_n[d]	M_w/M_n[d]	
1	**1/3**	30	54	20,100	2.32	98,000	2.78	1.05
2	**2/3**	30	66	11,700	2.41	36,700	3.16	1.53
3	**1/4**	60	52	3500	1.28	14,600	2.15	0.81
4	**2/4**	60	48	8600	1.94	15,400	2.59	1.34

[a] Conditions: $[\mathbf{1}]_0 = [\mathbf{2}]_0 = 60$ mM, $[\mathbf{3}]_0 = [\mathbf{4}]_0 = 40$ mM, $[PdCl_2(PPh_3)_2] = 1$ mM, $[CuI] = 4$ mM, $[PPh_3] = 6$ mM in toluene/Et_3N = 9:1 (v/v), 72 h.

[b] Acetone-insoluble part.

[c] Determined by GPC-UV, eluted with THF, polystyrene calibration.

[d] Determined by GPC-RALLS, eluted with THF.

[e] Calculated by ^{1}H NMR using Eqs. (1) and (2).

RALLS were in the range of 14,600–98,000. The RALLS-determined molecular weights were apparently larger than those determined by GPC-UV with polystyrene calibration, as commonly observed in the cases of non-linear polymers such as star-shaped, dendritic, and hyperbranched polymers [17]. *N*-Octadecylated poly(**1/3**) and poly(**1/4**) were soluble in common organic solvents including $CHCl_3$, THF, CH_2Cl_2 and toluene, and insoluble in acetone, MeOH and *n*-hexane. On the other hand, *N*-octylated poly(**2/3**) and poly(**2/4**) were soluble in $CHCl_3$ and THF, partly soluble in CH_2Cl_2 and toluene, and insoluble in acetone, MeOH and *n*-hexane, indicating that the longer alkyl chain was effective to enhance the solubility of the polymers.

3.2. Polymer structure

The polymer structures were examined by IR and ^{1}H NMR spectroscopies. No absorption was observed around 3300 and 2102 cm^{-1} attributable to the stretching vibration of ≡C–H single and ArC≡CH triple bonds in the IR spectra of poly(**1/3**)–poly(**2/4**), while an absorption peak was observed at 2210 cm^{-1} attributable to the stretching vibration of ArC≡CAr′ triple bond. In the ^{1}H NMR spectra of the polymers, no signal was observed around 3.0 ppm assignable to acetylenic proton of the monomers as shown in Fig. 1. All these results clearly indicate that Sonogashira coupling polymerization took place to form the polymers composed of –C≡C– linkage.

To gain more insights into the polymer structures, the unit ratios (*r*) of A_2-monomers **1** and **2** versus B_3-monomers **3** and **4** were calculated based on the integration ratios between the *N*–CH_2 proton signal around 4.2 ppm (peak b in Fig. 1) and aromatic proton signals at 7.0–8.3 ppm. In the case of poly(**1/3**) and poly(**2/3**), *r* can be calculated according to Eq. (1).

$$(3r+6)/r = A_{\mathrm{Ar}}/A_{N\mathrm{-CH_2}} \tag{1}$$

where *r* is A_2-monomer unit/B_2-monomer unit (mol/mol), A_{Ar} is the integration area of aromatic proton signals, and $A_{\mathrm{N-CH_2}}$ is the integration area of *N*–CH_2 proton signals.

In the case of poly(**1/4**) and poly(**2/4**), *r* can be calculated according to Eq. (2).

$$(6r+3)/2r = A_{\mathrm{Ar}}/A_{N\mathrm{-CH_2}} \tag{2}$$

The calculated results of the polymers are given in Table 1. We could not determine the degree of branching by NMR spectroscopy, because there were no appropriate signals available to distinguish dendritic, linear, and terminal units, which are necessary to determine the parameter [18]. Since no signal of a terminal acetylene proton was observed in the ^{1}H NMR spectra, the completion of the end-capping reaction was confirmed.

3.3. Polymer properties

Fig. 2A depicts the UV–vis spectra of poly(**1/3**)–poly(**2/4**) measured in $CHCl_3$. All the polymers exhibited absorption peaks at 310 and 350–370 nm attributable to carbazolylene and phenyleneethynylene moieties. The absorption peaks were red-shifted compared to those of **1** and **2** (290 and 350 nm). This fact means the extension of conjugation length upon transformation from the monomers to polymers. The UV–vis absorption band edges of poly(**1/3**) and poly(**2/3**) positioned at a longer wavelength than those of poly(**1/4**) and poly(**2/4**) indicate that the triphenylamine-based former two polymers have main chain conjugation longer than that of the latter two polymers.

Fig. 2B shows the fluorescence spectra of poly(**1/3**)–poly(**2/4**) excited at the absorption maxima. The polymer solutions emitted fluorescence, whose maximum wavelength was 420 nm upon excitation at 370 nm in the cases of triphenylamine-linked poly(**1/3**) and poly(**2/3**), and 375 nm upon excitation at 355 nm in the cases of benzene-linked poly(**1/4**) and poly(**2/4**). As summarized in Table 2, the fluorescence quantum yields of the present polymers ranged from 9 to 67% in $CHCl_3$, which were larger than those of polyacetylenes carrying carbazole moieties in the side chain [5]. However, they were smaller than those of poly(aryleneethynylenes) (up to 86%) [9]. Entanglement of polymer chains containing excited species may occur to cause intersystem crossing to some extent, but the concrete reason is unclear. The fluorescence quantum yields of poly(**1/4**) and poly(**2/4**) were much larger than those of poly(**1/3**) and poly(**2/3**). It is likely that triphenylamine-linked poly(**1/3**) and poly(**2/3**) were less rigid than benzene-linked poly(**1/4**) and poly(**2/4**), resulting in low quantum yields due to nonradiative decay [9]. It was also found that the fluorescence quantum yields of poly(**1/3**) and poly(**1/4**) were larger than those of the counterparts, poly(**2/3**) and poly(**2/4**), respectively. The presence of longer alkyl chains on the nitrogen atoms led to increase of the fluorescence quantum yields of the polymers.

Fig. 3 depicts the cyclic voltammetric (CV) curves of poly(**1/3**)–poly(**2/4**). The oxidation of poly(**1/4**) started at 0.85 V in the first scan and the potential shifted to a higher field as the CV scan was continued. It seems that a conducting polymer film was formed on the working electrode surface, and the film thickness gradually increased upon CV scanning. The potential shift provided the information on the increase of the electrical resistance in the polymer film. Over potential was presumably needed to overcome the resistance. The potential was somewhat higher than those of *N*-alkylcarbazole derivatives reported so far (0.7–0.8 V) [19]. On the other hand, the other polymers did not exhibit such a large shift of the initiation of oxidation potential. All the polymers showed obvious reduction peaks around 0.70 V, indicating that the present hyperbranched polymers containing carbazole moieties are electrochemically redox-active.

3.4. Solvent-induced aggregation

Several conjugated polymers show significant intermolecular interactions based on π stacking in the solid state [20]. Optical properties induced by this type of intermolecular interactions are explained by the exciton model, wherein

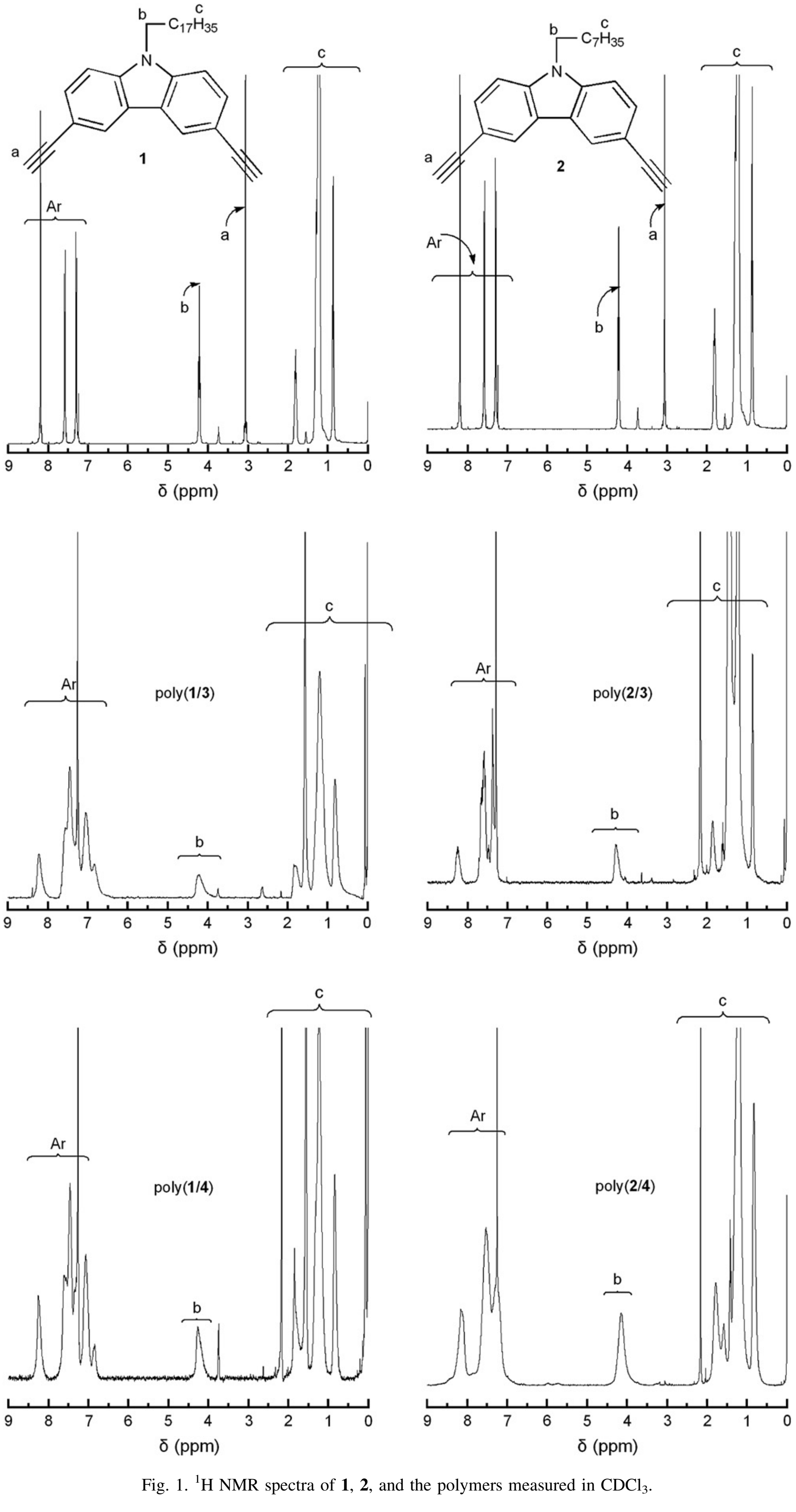

Fig. 1. ^{1}H NMR spectra of **1**, **2**, and the polymers measured in $CDCl_3$.

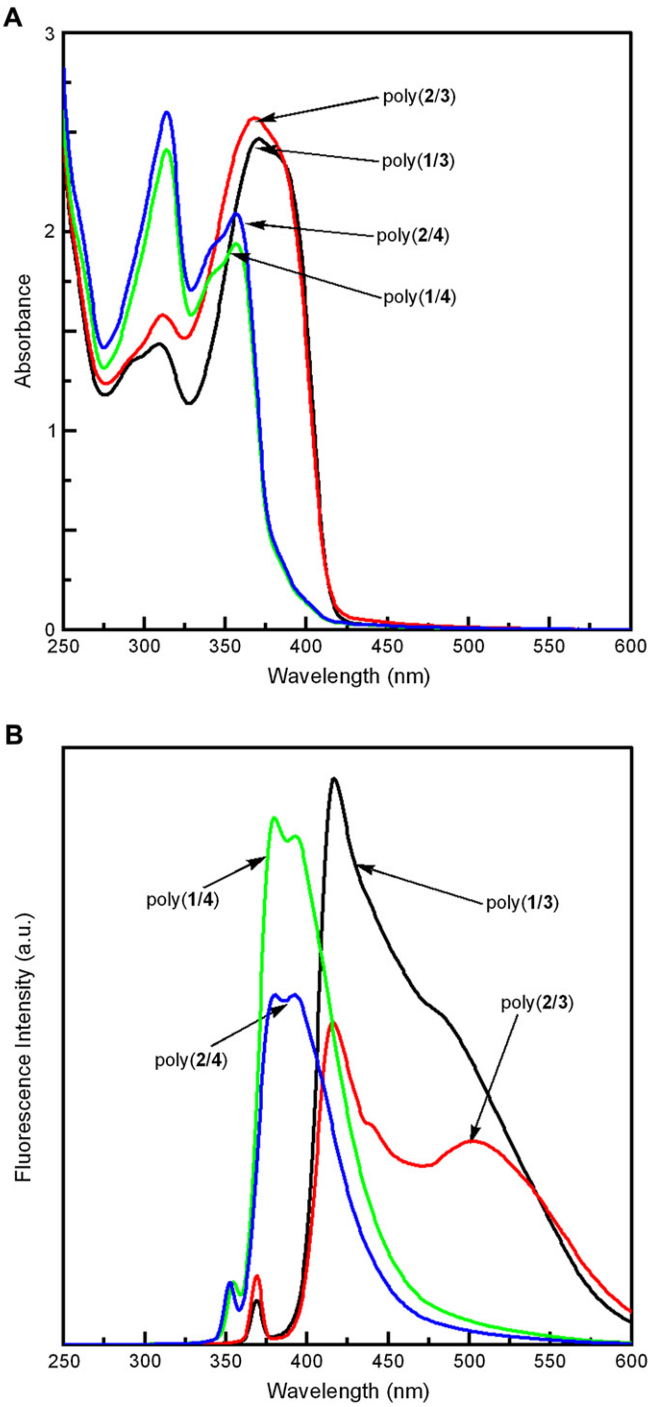

Fig. 2. UV–vis and fluorescence spectra of the polymers measured in $CHCl_3$. UV–vis spectra: $c = 0.1$ g/L; fluorescence spectra: poly(**1**/**3**) and poly(**2**/**3**) were excited at 370 nm, $c = 0.1$ g/L; poly(**1**/**4**) and poly(**2**/**4**) were excited at 355 nm, $c = 0.05$ g/L.

splitting (Davydov splitting) of an absorption band is induced by two orientations of molecular transition dipole moments, H-aggregates (parallel orientation of the molecules) and J-aggregates (head-to-tail orientation) [20]. The addition of nonsolvents to a polymer solution also possibly induces molecular aggregation.

Fig. 4 depicts the fluorescence spectra of the polymers measured in $CHCl_3$/MeOH mixtures. The fluorescence intensity around 420 nm tended to decrease upon raising MeOH content in the cases of triphenylamine-based poly(**1**/**3**) and poly(**2**/**3**). Simultaneously, the relative band intensity around 500 nm increased. The appearance of the red-shifted fluorescence band can be interpreted by the intermolecular aggregation and formation of excimers like in the film state.

Table 2
Fluorescence quantum yields of poly(**1**/**3**)–poly(**2**/**4**) measured in $CHCl_3$/MeOH

$CHCl_3$/MeOH (v/v)	Fluorescence quantum yield[a] (%)			
	Poly(**1**/**3**)[b]	Poly(**2**/**3**)[b]	Poly(**1**/**4**)[c]	Poly(**2**/**4**)[c]
10:0	14.8	9.0	66.8	50.0
9:1	16.7	9.2	72.0	60.6
7:3	15.0	5.2	68.3	53.2
5:5	11.4	4.5	55.0	49.6
3:7	9.2	4.0	44.0	45.0

[a] Determined based on carbazole.
[b] Concentration 0.1 g/L, excited wavelength 370 nm.
[c] Concentration 0.05 g/L, excited wavelength 355 nm.

Poly(**1**/**4**) and poly(**2**/**4**) also tended to decrease the fluorescence intensity around 400 nm upon the addition of MeOH to $CHCl_3$, while they did not show such excimer-based fluorescence as poly(**1**/**3**) and poly(**2**/**3**) did. Since the tri-arm benzene linker is rigid compared to the triphenylamine linker, excimer formation seems to be prevented in the cases of poly(**1**/**4**) and poly(**2**/**4**). This is supported by the experimental fact that the fluorescence of poly(**1**/**4**) and poly(**2**/**4**) is more stable than that of poly(**1**/**3**) and poly(**2**/**3**) toward MeOH addition. Table 2 summarizes the fluorescence quantum yields calculated from the curves in Fig. 4.

As described above, the polymers changed the optical properties upon aggregation, presumably governed by excitonic effects. The degree of fluorescence quenching of the present polymers upon MeOH addition was smaller than that of poly(*N*-octyl-2,7-carbazolediyl) [11]. It is considered that the present polymers change the conformation less easily due to the hyperbranched structure.

Fig. 5 shows the UV–vis and PL spectra of poly(**1**/**3**) measured in various solvents. The UV–vis spectral patterns were almost the same to one another irrespective of the solvents, while the peak top wavelengths and intensities were different, especially in CH_2Cl_2. The fluorescence quantum yield ranged from 13% (in toluene) to 35% (in CH_2Cl_2). This solvatochromism is probably caused by photoinduced intramolecular charge transfer in the excited state [21].

Fig. 6 depicts the *I*–*V* curve of an ITO/poly(**1**/**3**)/Au cell. The dark conductivity was calculated to be ca. 1.8×10^{-15} S/cm under an electric field of 10^3 V/cm. This value is about one order higher than that of poly(*t*-Bu_2CzPA) [22], presumably due to π conjugation of hyperbranched polymer. The longer alkyl chain on the carbazolyl group is probably effective for π stacking of carbazolylene moiety through hydrophobic interaction between alkyl chains. This results in higher dark conductivity of poly(**1**/**3**). Higher fluorescence quantum yields of the polymers with longer alkyl chain support this explanation. The current was twice as large under

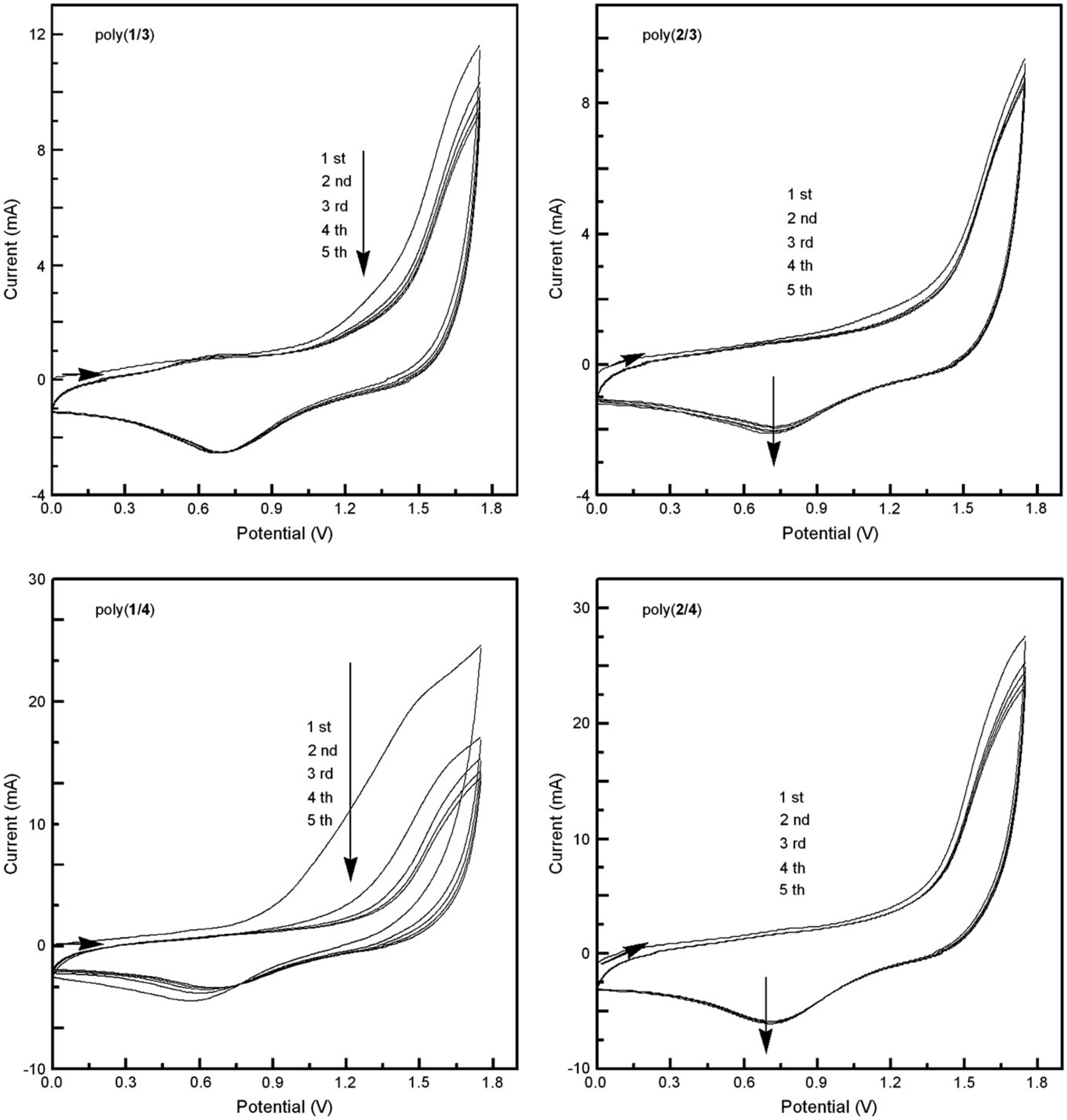

Fig. 3. Cyclic voltammograms of the polymers measured at a scan rate of 0.1 V/s versus Ag/Ag$^+$ in a CHCl$_3$ solution containing tetrabutylammonium perchlorate (0.1 M). Polymer concentration: 0.5 g/L.

photoillumination as in the dark. This proves that poly(**1/3**) exhibits photoconductivity. It has been reported that photocurrent/dark current ratio of polyacetylenes carrying carbazole moieties in the side chain is 10–50, which depends on the structure but is larger than that of poly(**1/3**) [5]. The dark current of poly(**1/3**) is comparable to that of polyacetylenes carrying carbazole moieties in the side chain. By taking the absorption edge and the low conductivity of both polymers, the carrier mobility is not so much different among them. Therefore, the difference in these photocurrents should be attributed to the number of photogenerated carriers. As mentioned above, poly(**1/3**) showed higher fluorescence quantum yield than polyacetylenes with carbazole pendants, suggesting that photogenerated holes should diminish in poly(**1/3**) by the effective quenching. It is assumed that poly(**1/3**), therefore, shows lower photoconductive properties. However, the results of Fig. 6 clearly indicate that the designed polymer works as an optoelectronic functional polymer.

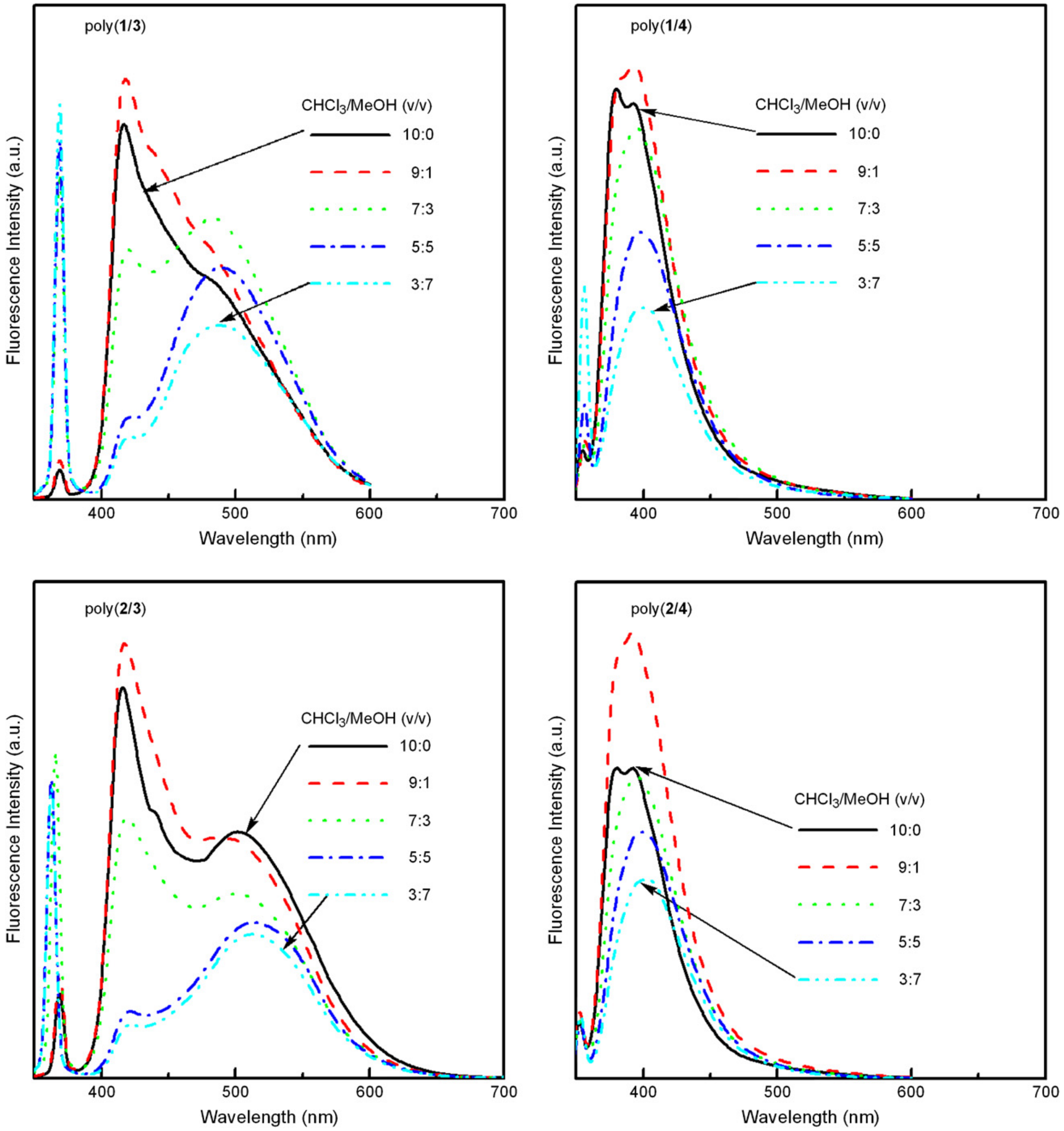

Fig. 4. Fluorescence spectra of the polymers measured in $CHCl_3$/MeOH with various compositions. Poly(**1/3**) and poly(**2/3**) were excited at 370 nm, $c = 0.1$ g/L; poly(**1/4**) and poly(**2/4**) were excited at 355 nm, $c = 0.05$ g/L.

4. Conclusions

In this article, we have demonstrated the synthesis of carbazole-based novel hyperbranched conjugated polymers linked with triphenylamine and benzene units. Solvent-soluble polymers with M_n ranging 3500–21,000 were successfully obtained by the polycondensation of diethynylcarbazoles with tris(4-iodophenyl)amine and 1,3,5-tribromobenzene in 48–66% yields. The UV–vis absorption of the polymers was red-shifted as compared to carbazole, indicating the extension of conjugation length. The fluorescence quantum yields of the polymers reached 67% in $CHCl_3$ at the maximum, which were larger than those of polyacetylenes carrying carbazole moieties in the side chains. The fluorescence quantum yields of poly(**1/3**) and poly(**1/4**) having longer *N*-alkyl chains were larger than those of poly(**2/3**) and poly(**2/4**), respectively. The degree of fluorescence quenching of the present polymers upon MeOH addition was smaller than the linear counterpart previously reported. The branched structure was effective to suppress the decay of fluorescence. CV study confirmed that the polymers were electronically redox-active. Poly(**1/3**) was proved to work as an optoelectronic functional

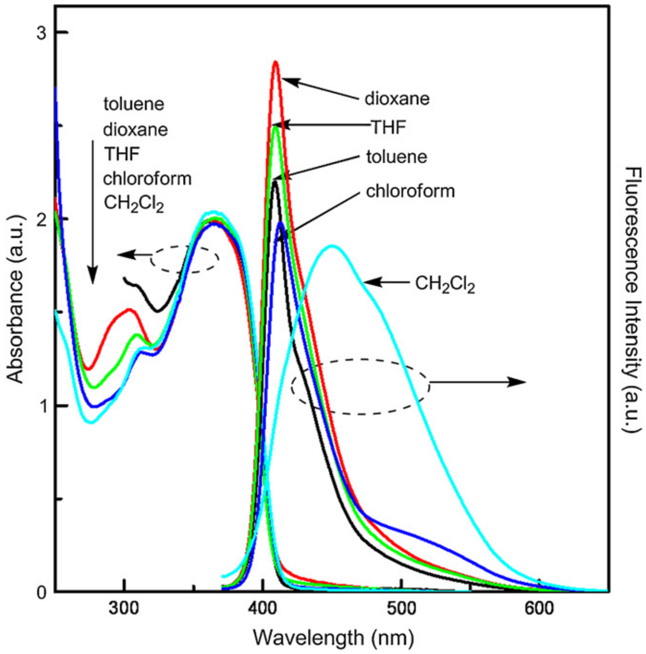

Fig. 5. Absorption and emission spectra of poly(**1**/**3**) measured in various solvents, $c = 0.1$ g/L; excitation wavelength: 370 nm.

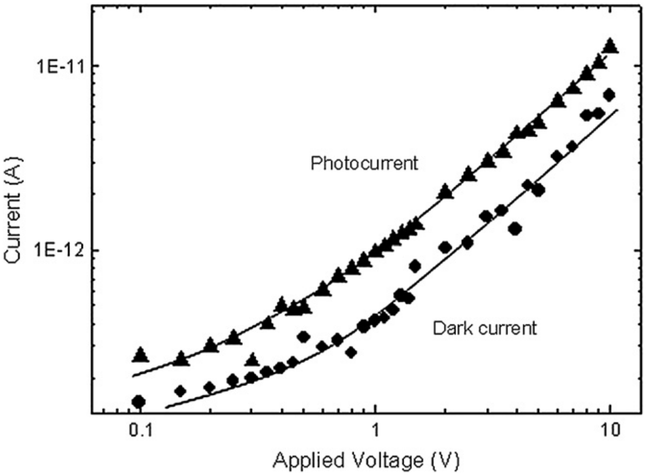

Fig. 6. Relationships between current and voltage applied to ITO/poly(**1**/**3**)/Au cells (effective electrode area 0.12 cm^2, thickness 6 μm) measured at room temperature under reduced pressure ca. 10^{-2} Torr.

polymer. The information obtained in this study may assist the rational design of tunable light-emitting materials based on carbazole-containing polymers.

Acknowledgments

This research was partly supported by a Grant-in-Aid for Science Research in a Priority Area ‘‘Super-Hierarchical Structures (No. 446)’’ from the Ministry of Education, Culture, Sports, Science and Technology, Japan. Jinqing Qu acknowledges the financial support from the Ministry of Education, Culture, Sports, Science, and Technology (Monbukagakusho), Japan. We would like to thank Professor Ben-zhong Tang for helpful discussion about solvatochromism.

References

[1] (a) Tani K, Matsumura K, Hori K, Tohda Y, Takemura H, Ohkita H, et al. Chem Lett 2002;934–5;
(b) Ohkita H, Ito S. J Phys Chem A 2002;106:2140–5;
(c) Tani K, Tohda Y, Takemura H, Ohkita H, Ito S, Yamamoto M. Chem Commun 2001;1914–5;
(d) Nakamura Y, Kaneko M, Yamanaka N, Tani K, Nishimura J. Tetrahedron Lett 1999;40:4693–6.

[2] (a) Morin JO, Leclerc M, Adès D, Siove A. Macromol Rapid Commun 2005;26:761–78;
(b) Grazulevicius JV, Strohriegl P, Pielichowski J, Pielichowski K. Prog Polym Sci 2003;28:1297–353;
(c) Akcelrud L. Prog Polym Sci 2003;28:875–962;
(d) Wang YZ, Epstein AJ. Acc Chem Res 1999;32:217–24.

[3] (a) Tang BZ, Chen HZ, Xu RS, Lam JWY, Cheuk KKL, Wong HNC, et al. Chem Mater 2000;12:213–21;
(b) Pui-Sze LP, Geng Y, Kwok HS, Tang BZ. Thin Solid Films 2000;363:149–51.

[4] Tabata M, Fukushima T, Sadahiro Y. Macromolecules 2004;37:4342–50.

[5] (a) Fulghum T, Abdul Karim SM, Baba A, Taranekar P, Nakai T, Masuda T, et al. Macromolecules 2006;39:1467–73;
(b) Sanda F, Kawasaki R, Shiotsuki M, Masuda T. Polymer 2004;45:7831–7;
(c) Sanda F, Kawaguchi T, Masuda T. Macromolecules 2003;36:2224–9;
(d) Sata T, Nomura R, Wada T, Sasabe H, Masuda T. J Polym Sci Part A Polym Chem 1998;36:2489–92;
(e) Nakano M, Masuda T, Higashimura T. Polym Bull 1995;34:191–7.

[6] (a) Jiang J, Jiang C, Yang W, Zhen H, Hung F, Cao Y. Macromolecules 2005;38:4072–80;
(b) Zhang ZB, Motonaga M, Fujiki M, McKenna CE. Macromolecules 2003;36:6956–8;
(c) Huang J, Niu Y, Yang W, Mo Y, Yuan M, Cao Y. Macromolecules 2002;35:6080–2;
(d) Morin JF, Leclerc M. Macromolecules 2002;35:8413–7;
(e) Morin JF, Leclerc M. Macromolecules 2001;34:4680–2;
(f) Zhang Y, Wada T, Sasabe H. J Polym Sci Part A Polym Chem 1996;34:2289–98.

[7] (a) Brizius G, Kroth S, Bunz UHF. Macromolecules 2002;35:5317–9;
(b) Beginn C, Grazulevicius JV, Strohriegl P. Macromol Chem Phys 1994;195:2523–9.

[8] Jung HK, Lee CL, Lee JK, Kim JK, Park SY, Kim JJ. Thin Solid Films 2001;401:111–7.

[9] Takihana Y, Shiotsuki M, Sanda F, Masuda T. Macromolecules 2004;37:7578–83.

[10] (a) Koren AB, Curtis MD, Kampf JW. Chem Mater 2000;12:1519–22;
(b) Politis JK, Somoza FB, Kampf JW, Curtis MD, Gonzalez RL, Martin DC. Chem Mater 1999;11:2274–84.

[11] (a) Belletête M, Bouchard J, Leclerc M, Durocher G. Macromolecules 2005;38:880–7;
(b) Li K, Wang Q. Macromolecules 2004;37:1172–4;
(c) Bouchard J, Belletête M, Durocher G, Leclerc M. Macromolecules 2003;36:4624–30.

[12] (a) Li Z, Qin A, Lam JWY, Dong Y, Dong Y, Ye C, et al. Macromolecules 2006;39:1436–42;
(b) Ma H, Li S, Luo J, Suresh S, Liu L, Kang SH, et al. Adv Funct Mater 2002;12:565–74;
(c) Robinson BH, Dalton LR. J Phys Chem A 2000;104:4785–95;
(d) Dalton LR, Steier WH, Robinson BH, Zhang C, Ren A, Garner S, et al. J Mater Chem 1999;9:19–24.

[13] (a) Häußler M, Tang BZ. Adv Polym Sci 2007;209:1–58;
(b) Kraemer M, Kopaczynska M, Krause S, Haag R. J Polym Sci Part A Polym Chem 2007;45:2287–303;
(c) Reisch A, Komber H, Voit B. Macromolecules 2007;40:6846–58;

(d) Komber H, Stumpe K, Voit B. Macromol Chem Phys 2006;207:1814–24;
(e) Sunder A, Mülhaupt R, Haag R, Frey H. Adv Mater 2000;12:235–9;
(f) Sunder A, Heinemann J, Frey H. Chem Eur J 2000;6:2499–506.
[14] (a) Paul GK, Mwaura J, Argun AA, Taranekar P, Reynolds JR. Macromolecules 2006;39:7789–92;
(b) Dong H, Zheng R, Lam JWY, Ussler MH, Qin A, Tang BZ. Macromolecules 2005;38:6382–91;
(c) Sun M, Li J, Li B, Fu Y, Bo Z. Macromolecules 2005;38:2651–8;
(d) Menon A, Galvin M, Walz KA, Rothberg L. Synth Met 2004;141:197–202.
[15] (a) Shirota Y. J Mater Chem 2005;15:75–93;
(b) Saragi TPI, Fuhrmann-Lieker T, Salbeck J. Synth Met 2005;148:267–70;
(c) Sonntag M, Kreger K, Hanft D, Strohriegl P, Setayesh S, de Leeuw D. Chem Mater 2005;17:3031–9;
(d) Petrella A, Cremer J, De Cola L, Bäuerle P, Williams RM. J Phys Chem A 2005;109:11687–95.
[16] (a) Li ZA, Di CA, Zhu Z, Yu G, Li Z, Zeng Q, et al. Polymer 2006;47:7889–99;
(b) Wu CW, Lin HC. Macromolecules 2006;39:7232–40;
(c) Liu XM, Xu J, Lu X, He C. Macromolecules 2006;39:1397–402;
(d) Liu XM, Xu J, Lu X, He C. Org Lett 2005;7:2829–32.
[17] Muchtar Z, Schappacher M, Deffieux A. Macromolecules 2001;34:7595–600.
[18] Hawker CJ, Lee R, Fréchet MJ. J Am Chem Soc 1991;113:4583–8.
[19] (a) Wei ZH, Xu JK, Nie GM, Du YK, Pu SZ. J Electroanal Chem 2006;589:112–9;
(b) Chiu KY, Su TX, Li JH, Lin TH, Liou GS, Cheng SH. J Electroanal Chem 2005;575:95–101.
[20] (a) Pålsson LO, Wang C, Russel DL, Monkman AP, Bryce MR, Rumbles G, et al. Chem Phys 2002;279:229–37;
(b) Jenekhe SA, Lu L, Alam M. Macromolecules 2001;34:7315–24;
(c) Theander M, Anderson MR, Inganäs O. Synth Met 1999;101:331–2.
[21] Qin A, Jim CKW, Lu W, Lam JWY, Haussler M, Dong Y, et al. Macromolecules 2007;40:2308–17.
[22] Sanda F, Nakai T, Kobayashi N, Masuda T. Macromolecules 2004;37:2703–8.